THERMAL CONDUCTIVITY OF ULTEM™/CARBON NANOFILLER BLENDS

S. Ghose[1], K.A. Watson[2], D.M. Delozier[2], D.C. Working[3], J.W. Connell[3], J.G. Smith Jr.[3], Y.P. Sun[4] and Y. Lin[4]

[1]NASA Postdoctoral Fellow at NASA LaRC, Hampton, VA 23681-2199

[2] National Institute of Aerospace, Hampton, VA 23666-6147

[3]NASA Langley Research Center, Hampton, VA 23681-2199

[4]Dept of Chemistry, Clemson University, Clemson, SC 26934-0973

Abstract

In an effort to improve polymer thermal conductivity (TC), Ultem™ 1000 was compounded with nano-fillers of carbon allotropes. Ultem™ 1000 was selected since it is both solution and melt processable. As-received and modified multiwalled carbon nanotubes (MWCNTs), vapor grown carbon nanofibers (CNF) and expanded graphite (EG) were investigated. MWCNTs were modified by functionalizing the surface through oxidization with concentrated acids, mixing with an alkyl bromide, and addition of alkyl and phosphorus compounds after initial treatment with n-butyl lithium. Functionalization was performed to improve the TC compatibility between the resin and MWCNTs. It was postulated that this may provide an improved interface between the MWCNT and the polymer which would result in enhanced TC. The nano-fillers were mixed with Ultem™ 1000 in the melt and in solution at concentrations ranging from 5 to 40 wt%. Ribbons were extruded from the blends to form samples where the nano-fillers were aligned to some degree in the extrusion direction. Samples were also fabricated by compression molding resulting in random orientation of the nano-fillers. Thermal properties of the samples were evaluated by Differential Scanning Calorimetry (DSC) and Thermal Gravimetric Analyzer (TGA). Tensile properties of aligned samples were determined at room temperature. The specimens were cut from the ribbons in the extrusion direction; hence the nano-fillers are somewhat aligned in the direction of stress. Typically it was observed that melt mixed samples exhibited superior mechanical properties compared to solution mixed samples. As expected, increased filler loading led to increased modulus and decreased elongation with respect to the

neat polymer. The degree of dispersion and alignment of the nano-fillers was determined by high-resolution scanning electron microscopy (HRSEM). HRSEM of the ribbons revealed that the MWCNTs and CNFs were predominantly aligned in the flow direction. The TC of the samples was measured using a Nanoflash™ instrument. Since the MWCNTs and CNF are anisotropic, the TC was expected to be different in the longitudinal (parallel to the nanotube and fiber axis) and transverse (perpendicular to the nanotube and fiber axis) directions. The extruded ribbons provided samples for transverse TC measurements. However, to determine the TC in the longitudinal direction, the ribbons needed to be stacked and molded under 1.7 MPa and 270 °C. Samples were then obtained by cutting the molded block with a diamond saw. The largest TC improvement was achieved for aligned samples when the measurement was performed in the direction of MWCNT and CNF alignment (i.e. longitudinal axis). Unaligned samples also showed a significant improvement in TC and may be potentially useful in applications when it is not possible to align the nano-filler. The results of this study will be presented.

Corresponding author: John W. Connell, john.w.connell@nasa.gov, 1-757-864-4264

1. INTRODUCTION

Combining polymers with an organic or inorganic phase to produce a polymer composite is common in the production and processing of modern plastics. Recently, the use of nanoscale fillers to prepare polymer nanocomposites (PNC) have been investigated to augment the properties of polymers. PNCs are commonly defined as the combination of a polymer matrix resin and inclusions that have at least one dimension in the nanometer size range [1]. PNCs exhibit significant enhancements in certain properties at a far lower concentration than their conventional micro or macro counterparts. Layered clay, EG, CNF and carbon nanotubes (CNTs) are some of the common nanoparticles used in making PNCs.

Carbon nanofibers (CNF) are widely used as reinforcements for polymers in numerous high-technology applications because of their excellent electrical and thermal properties and high specific tensile strength and modulus [2]. Other benefits provided by CNFs include improved heat distortion temperatures and increased electromagnetic shielding. CNFs have been used as reinforcements for various thermoplastics like polyethylene [3], polypropylene [4,5], polycarbonate [6], nylon [7] and poly (methyl methacrylate) [8]. These highly graphitic fibers are produced by a catalytic vapor deposition process and have a wide range of morphologies, from disordered bamboo-like formations [9] to highly graphitized "stacked-cup" structures where conical shells are nested within one another [10]. Additionally, CNFs are generally more economically attractive than CNTs because of lower manufacturing costs.

Graphite is another material that is commonly used as a filler in polymers. Graphite is one of the stiffest materials found in nature with a Young's modulus of ~1060 MPa and also has excellent thermal and electrical properties. However, utilizing graphite, which exists in large stacks of graphene sheets, necessitates a prior expansion and exfoliation of the graphene layers to obtain particles with nanometer dimensions. With surface treatment of EG, its dispersion in a polymer matrix results in composites with excellent mechanical and electrical properties and high TC. In addition, the material is presently two orders of magnitude less expensive than CNTs [11]. Electrically conductive nanocomposites were prepared by solution intercalation and master batch melt mixing of high density polyethylene (HDPE)/maleic anhydride grafted polyethylene/EG [12]. HDPE was also reinforced with EG and untreated graphite by a melt compounding process

that improved electrical and mechanical properties of the EG composite [13]. EG has also been made by oxidation of natural graphite followed by thermal expansion and then poly(styrene-co-acrylonitrile)/EG composite sheets have been prepared [14]. Poly-methylmethacrylate/EG composites prepared by solution blending methods [15] and aromatic polydisulphide/EG nanocomposites prepared by solution method and hot molding [16] showed good mechanical and electrical properties. The dynamic mechanical and thermal properties of phenylethynyl-terminated polyimide composites reinforced with EG nanoplatelets have also been studied [17].

Carbon nanotube (CNT)-based composites are being studied intensively due to the unique physical/mechanical properties of CNTs. CNTs are thought of as the ultimate carbon fibers, and are expected to have high mechanical and electrical properties and ultra high TC [18, 19]. When CNTs are dispersed in polymeric materials, an interconnecting network is formed which provides a conductive pathway for electrical and/or thermal current to flow. In electrical conductivity the mechanism involves a flow of electrons whereas for TC the process of conduction occurs via transfer of phonons. However, one of the problems impeding the full realization of CNT properties in composites has been dispersability. Various methods have been attempted for achieving good dispersion of CNTs in the polymer. They include the preparation of the polymer in the presence of CNTs under sonication [20], the use of alkoxysilane terminated amide acid oligomers to disperse the CNTs [21], melt mixing [22] and shear mixing [23]. Other methods include use of surfactants and covalent functionalization of various groups. Covalent functionalization has been achieved through either carboxylic moieties generated on the CNT surface or by other chemistries providing covalent attachment [24].

Theory predicts the TC (κ) of CNTs at room temperature is as high as ~6600 W/mK [25]. The experimental value of 3000 W/mK for the thermal conductivity of an individual multiwalled carbon nanotube (MWCNT) at room temperature has been reported [26]. This value is significantly higher than that of known thermally conducting materials like diamond (up to 2300 W/mK) and graphite (up to 1960 W/mK). The prominent thermal properties of CNTs have made them promising materials for future applications as thermal management materials. Hence it is reasonable to study the TC applications of CNTs. Enhancement of TC has been observed in CNT

suspensions [27-28]. It is interesting to note that in the case of CNT suspensions, the measured TCs are generally greater than the theoretical predictions made with conventional heat conduction models. It has been shown in the case of single wall carbon nanotubes (SWCNTs) that TCs show a peaking behavior before falling off at higher temperatures due to Umklapp scattering [29]. In the case of ordinary carbon-carbon composites, there is a larger mean free path and less phonon-phonon Umklapp scattering causing the TC to increase linearly with heat treatment temperature [30]. However in PNCs, the improvement in TC has always been lower than the rule-of-mixture values. In addition to the dispersability issue, another reason that anticipated TC enhancements are not realized is that of thermal interface resistance or Kapitza resistance [31]. This resistance is related to the heat flow barrier between the two phonon spectra and weak contact at the interface, both of which lead to phonon backscattering. One method of reducing this interface problem is by covalent attachment of the CNTs to the matrix [32]. By molecular dynamics simulation on SWCNTs it was found that functionalization with octane on one of out of 15 CNT carbon atoms (~7% functionalization based on the model) reduced the thermal interface resistance by more than 3x. However, it was also mentioned that these attachments can in themselves act as phonon scattering centers and reduce the CNT conductivity.

ULTEM™ was chosen as the host resin for trials with the various nanoparticles because the resin is an amorphous thermoplastic polyetherimide offering good melt processability, outstanding high heat resistance, high strength, modulus and broad chemical resistance. For example, SWCNTs have been incorporated (up to 1% by weight) into ULTEM™ and melt processed to yield fibers [33]. Although the melt process was not optimized to fully disperse and align the SWCNTs some improvements in mechanical properties were achieved.

Melt compounding was chosen as the method to disperse the nanoparticles in ULTEM® because it involves high shear mixing which helps to disentangle the nanoparticles and disperse them uniformly within the matrix. Melt mixing was followed by extrusion in the preparation of some of the samples described herein. The process of extruding the nanocomposite through a suitable die and subsequent drawing led to continuous ribbons of nanocomposites with substantial orientation of the nanoparticles in the flow direction. The samples were characterized using differential scanning calorimetry, thermogravimetric analysis, high resolution scanning electron

microscopy, mechanical tester and thermal conductivity analyzer. The preparation and characterization of samples containing various loadings of CNTs, CNFs and EGs are discussed.

2. EXPERIMENTAL

2.1 Materials Ultem™ 1000, a melt processable polyimide obtained from GE Plastics, was chosen as the polymer matrix and was used as received. MWCNTs, VGE-S12 and VGE-S16, were procured from the University of Kentucky. CNF, Pyrograph – III - PR-24 HHT was obtained from Applied Sciences, Inc and EG (Grade 3775) was received from Asbury Carbons. The graphite already had the galleries expanded by first treating with sulfuric acid and then rapidly heating the sample to 900 ºC. The expansion of the graphite was expected to facilitate exfoliation during melt mixing. n-Butyl lithium (2.5 M in hexanes) and 1-bromododecane were obtained from Acros. Anhydrous tetrahydrofuran (THF) was obtained from Fisher. All other chemicals were obtained from commercial sources and used as received.

2.2 MWCNT modification

To a flame dried 3 necked 250 mL round-bottom flask equipped with a nitrogen inlet, pressure equalizing funnel, mechanical stirrer and a drying tube, was charged 0.8330 g of VGE S12. The MWCNTs were flame dried under nitrogen and allowed to cool to room temperature under nitrogen, then 30 mL of anhydrous THF was added via cannula addition. The mixture was sonicated in an ULTRAsonik 57x bath at room temperature at ~50% power and degas levels for ~ 0.5 hr. The mixture was then cooled in a dry ice-acetone bath to ~ -78°C. n-Butyllithium (20 mL) was added dropwise over ~0.25 h. The mixture was stirred at temperature for ~ 0.75 h under nitrogen. Then 1-bromododecane (8.4 g) dissolved in anhydrous THF (35 mL) was added dropwise over ~ 2 h. The stirred mixture was allowed to warm to room temperature overnight. The mixture was cooled in an ice bath and ~100 mL water and ~ 4 mL concentrated hydrochloric acid was added to the stirred mixture. The mixture was allowed to warm to room temperature with stirring. Upon addition of the aqueous acidic solution, the product separated from solution. The product was recovered by vacuum filtration, washed in stirred warm water (3x), and washed with diethyl ether (3x). After air drying at room temperature, the material was dried in a forced air oven at 110°C overnight. The yield was 0.91 g.

2.3 Processing of Ultem™ 1000 with nanofillers Ultem™ 1000 was compounded with MWCNTs, CNFs and EGs in a 30 cc internal mixer (Plasticorder PL2000, Banbury) for 3 h at 25 rpm, 325 °C under N_2 purge. MWCNTs - 5, 10 and 20 wt%, CNFs - 20, 30 and 40 wt%, and EGs - 20, 30, 40 and 50 wt% were added to the polymer. During mixing the torque produced was used to calculate the viscosity of the sample. Upon completion of mixing the material was ground in a Mini-Granulator (Kayeness, Inc) using a 5.5 mm screen. Samples were extruded through a Laboratory Mixing Extruder (#LME, Dynisco, Inc) at a barrel temperature of 215 °C and a die temperature of 365 °C for the CNF sample, a barrel temperature of 215 °C and a die temperature of 360 °C for the MWCNT sample and a barrel temperature of 190 °C and a die temperature of 350 °C for the EG sample. The dimensions of the die were 0.38 mm x 19.1 mm. The samples were extruded in the form of a continuous ribbon that were 0.1-0.5 mm thick, 10-15 mm wide and several meters in length. Once extruded, the ribbons were cut into pieces approximately 2 cm x 2 cm. They were then stacked on one side of a mold 9 cm x 2 cm x 3 cm (i.d.) and the remainder of the mold filled with Ultem™ 1000 pellets. The stacked ribbons were compression molded at 270 °C, 1.72 MPa for 3 h. The molded samples were then sliced using an Isomet low speed saw with a diamond wafering blade 10.2 cm diameter and 0.3 mm thick with 15 HC diamond (Buehler Ltd). Unoriented samples were made using a Laboratory Mixing Molder (#LMM Dynisco, Inc) and a rectangular mold (1.52 mm x 38.1 mm x 1.27 mm). A rough blend of materials was added to the mixing bowl of LMM kept at 360 °C and maintained there for 0.5 h. It was then dynamically pressed at a rotational speed of 100% of ram-motor capacity and then static pressed to degas, before passing through the nozzle orifice (~1.6mm) into the rectangular mold kept at 360 °C. The material was then manually compressed at a pressure of ~ 4.5 kN and set under pressure from the ram while being air cooled.

2.4 Solution mixing of Ultem™ 1000 with nanofillers Solution mixing of the Ultem™ 1000 with MWCNTs was conducted in N,N-dimethylacetamide (DMAc) using a polyimide dispersant, sonication and mechanical (low shear) mixing. The chemical structure of the dispersant is depicted in Figure 1. This polymer aids in the dispersal of the MWCNTs into the host polymer. The experimental procedure is as follows: Into a 500 mL round-bottom flask was placed VGE-S12 MWCNT (0.75 g) and DMAc (285 mL). This suspension was sonicated for 0.5 h in a Bransonic sonicator. The polyimide dispersant (0.75 g) was added to the suspension and

sonicated for 0.5 h with the MWCNTs. Ultem™ 1000 was then added in three additions of 5 g each with 0.5 h of sonication between each addition. The mixture was then subjected to overhead stirring for 16 h followed by precipitation into water. The powder was washed one time with 2 L of water and then dried at 100 ºC for 16 h at ambient pressure. The powder was then heated to 150 ºC for 4 h. For CNF samples, approximately 17 g of neat Ultem™ was dissolved in 150 mL hot DMAc. In a separate flask, the required amount of CNF was sonicated in 150 mL DMAc for 1 h and the suspension subsequently added to the Ultem™ solution. The mixture was stirred at room temperature for 3 h. The mixture was then poured into a blender containing water and the product collected via vacuum filtration. The product was washed several times in hot water and dried in an air oven at 125 °C for a minimum of 48 h.

2.5 Characterization Differential scanning calorimetry (DSC) was performed on ribbon samples obtained from extrusion in a sealed aluminum pan using a Shimadzu DSC-50 thermal analyzer at a heating rate of 20 ^{o}C/min with the glass transition temperature (T_g) taken as the mid-point of inflection of the differential heat flow (ΔH) versus temperature curve. Thermogravimetric analysis (TGA) was performed in air (flow rate – 50 mL/min) on powdered samples using an Auto TGA 2950HR (TA Instruments, DE). The samples were heated at 20 ^{o}C/min to 100 ^{o}C, held for 0.5 h to drive off any moisture, and heated to 600 ^{o}C at a rate of 2.5 ^{o}C/min. HRSEM images were obtained using a Hitachi S-5200 field emission scanning electron microscope (FE-SEM) equipped with a "through-the-lens" secondary electron detector. Thin-film tensile properties were determined according to ASTM D882 using either four or five specimens (0.51 cm wide) per test conditions using an Eaton Model 3397-139 11.4 kg load cell on a Sintech 2 test frame. The test specimen gauge length was 5.1 cm and the crosshead speed for film testing was 0.51 cm/minute. Thermal conductivity of the molded samples as well as ribbons was measured using a Netzsch LFA 447 NanoFlash according to ASTM E1461. Samples sizes of 1 cm x 1 cm were sprayed with a thin layer of graphite (for uniform thermal adsorption), which may be easily rinsed away by solvent (e.g., methanol). Pyrex (TC ~ 1.09 W/mK, Cp ~ 0.76 J/gk) was used as the reference.

3. RESULTS AND DISCUSSION

3.1 Modification of MWCNTs MWCNTs obtained from the University of Kentucky (VGE-S12) were treated under the various reaction conditions described in Table 1. The reaction was worked-up in normal fashion and the product dried at ~110°C in flowing air. The mass increased for A and B on the order of ~9.6 and ~15%. This increase was supported by TGA, where the % weight loss was taken prior to the onset of rapid degradation. Additional analysis of A by TGA/MS at a heating rate of 10°C/min revealed that the degradation products were carbon chains about 4 carbons long. No mass gain was observed for C and D where the n-butyl-lithium and the 1-bromododecane was left out of the reaction, respectively. The TGA curve for C, where the 1-bromododecane was left out of the reaction, was comparable to that of the pristine tubes (VGE-S12). Even though D did not exhibit a mass increase, the TGA curve showed a ~ 5% weight loss prior to the onset of rapid degradation. When diphenylphosphinic chloride (E) was substituted for 1-bromododecane, the MWCNTs became more thermally stable. The onset temperature of rapid degradation increased from 455°C for VGE-S12 to 514°C for E. This was not expected since phosphine oxide groups tend to increase the thermal stability of a material. By TGA, there was ~3% weight loss by 514°C for E that is presumably attributable to the diphenylphosphine oxide moiety. During the reaction work-up and after air drying the modified tubes displayed an adverse affinity to water. The modified MWCNTs floated on the water surface and did not settle out even after centrifugation. The pristine tubes however did settle out of water as expected. An exception was E containing the phosphine oxide group which settled out of water. The modified MWCNTs were further characterized by DSC. The modified tubes (A) showed melting transitions at 45 and 113°C while the pristine tubes had exhibited no transitions. Endotherms were observed at 99 and 112 °C for B (scale-up of A). After cooling to room temperature from 300°C, the endotherms were 86 and 108°C. No transitions were observed for C and D where one of the reaction components was left out. The phosphine oxide bearing material (E) exhibited broad endotherms at 253 and 258°C which were not observed upon a subsequent heating. Elemental analysis of the modified tubes is presented in Table 1. For A and B, residual bromine and lithium were present. These elements were present in very minor amounts for C and D, where one of the components was left out of the reaction. This was surprising given that the same work-up conditions were employed. 1-Bromododecane contains 32.1% Br. Based on these results, ~ 6 and 15% 1-bromododecane may be presumably present in

A and B, respectively. A small amount of lithium was present in E. The phosphorus present in E can be attributed to ~2.7% diphenylphosphine oxide in the sample.

3.2 Processing of Ultem™/nanofillers The torque values were obtained during mixing in the Plasticorder and were used to calculate the melt viscosities of the samples. Table 1 denotes the calculated melt viscosities of the various samples at a shear rate of 92.5 sec^{-1} and a temperature of 325 ° C. It was found that some samples (40 wt% CNF, 50 wt% EG) could not be extruded into ribbons. The difficulty in extruding these samples was due to either their high melt viscosity or the increased thermal conductivity that led to additional heating in the feeding region of the extruder. Figure 2 shows a picture of a typical extruded ribbon. The primary purpose of extrusion was to try and align the nanofillers in the direction of flow. Stacked ribbons were molded and samples were obtained by cutting the molded block in the direction of the dotted line in Figure 3 using a diamond saw. In this way samples were obtained with alignment both parallel and perpendicular to the direction of conductivity measurement.

3.3 HRSEM of extruded ribbons Figure 4(a) shows the image of the 5 wt% MWCNT melt mixed ribbon while Figure 4(b) shows the solution mixed ribbon with the same concentration of MWCNTs. In both cases, it is observed that the MWCNTs are aligned in the direction of flow (indicated by the arrow). Figures 5(a), (b) and (c) show the alignment at higher MWCNT loading and in CNFs. Figure 5(d) shows the face view of ULTEM™ + 5 wt% MWCNT sample. The bumps on the surface indicate the nanotubes in the matrix that are aligned perpendicular to the surface of the sample. HRSEM images were obtained for the 40 wt% EG extruded ribbon (Figure 6). The graphite platelets were visible at high voltages. The platelets vary in size but are all under 1 micron in one dimension. The platelets appear to be very thin which indicates that exfoliation is taking place during the melt mixing. The particles appeared well dispersed throughout the polymer.

3.4. Mechanical properties of extruded ribbons Mechanical properties were measured on Ultem™/nanofiller composites with the results shown in Table 2. The strips used for testing were cut from ribbons that were prepared from extrusion; hence the nanofillers are somewhat in alignment in the direction of the stress. The 5 wt% MWCNT solution-mixed sample and the 40

wt% EG melt mixed sample did not provide ribbons of sufficient quality for mechanical testing. The other results should be viewed with care because the measurement of the ribbon thickness is not accurate due to uneven ribbon surfaces. The sample with 10 wt% MWCNT solution-mixed method is an example, where the measured thickness of the ribbon is greater than the "average" thickness of the ribbon, resulting in depressed mechanical properties. Typically it has been observed that the melt mixed samples exhibited superior mechanical properties, both modulus and strength, compared to the solution mixed samples. As expected, with increased filler loading level, the modulus increased and the elongation decreased.

3.5 Thermal characterization of extruded ribbons Table 3 denotes the T_gs of the various samples. In the case of MWCNT filled samples, the solution mixed composites exhibited a sharp decrease in T_gs for the 10 and 20 wt% loadings. The melt-mixed composites had negligible changes in T_gs. But in the cases of CNFs and EGs, samples showed very little change in T_gs. The addition of nanofillers improved the temperature of 5 wt% loss as determined by TGA. Neat Ultem™ lost 5 wt% at ~ 480 °C while the filled samples lost the same weight at temperatures > 500 °C. No significant differences in thermo-oxidative stability were observed for the melt-mixed and solution-mixed samples.

3.6 Thermal conductivity measurements Since the structure of nanotubes is anisotropic in space, the electrical and thermal properties should be different in the longitudinal (parallel to nanotube axis) and transverse (perpendicular to nanotube axis) directions. There have been a few reports on the use of dispersed CNTs as thermally conducting fillers in polymer composites and certain enhancements in TC were observed [25, 34]. However, the enhanced values are typically below those predicted by the rule of mixtures. One probable reason for this is the existence of interface thermal resistance between the overlaps in the CNT passage leading to a rapid increase in overall thermal resistance [35]. Huang et al. [34] proposed a composite structure where all the CNTs embedded in the matrix are aligned from one surface to the opposite side with all the CNT surfaces revealed on both surfaces. This leads to high TC since the CNTs form ideal thermally conducting pathways. Low thermal interface resistances can also be expected as the protruding tips would ensure better thermal contact. It has been reported that alignment of nanofillers in the polymer matrix leads to enhancement of TC [30, 36]. Based on the literature survey to date, it

was decided to process samples with significant nanofiller alignment and measure TC both in the direction and perpendicular to the direction of alignment (nanotube axis).

Three types of Ultem™/nanofiller samples were measured for TC. These were the extruded ribbon, molded samples cut perpendicular to flow direction, and samples with no alignment. For the extruded ribbons the TC was measured perpendicular to the direction of nanotube alignment. Table 4a denotes the values for neat Ultem™ and Ultem™/nanofiller samples. With the exception of the 10 wt% MWCNT sample, the solution mixed ribbons had a slightly higher TC than the melt mixed ones. The TC increased with increase in loading level of nanofillers. The highest TC was observed in the 30 wt% CNF samples and the conductivity increased by 180% with respect to the neat material. The second set of samples was the molded samples where the TC was measured in the direction of nanofiller alignment. Table 4b shows the values for the neat molded sample as well as Ultem™/nanofiller samples. This data has also been shown in a plot (Figure 7). In this case the melt-mixed samples showed a higher TC compared to solution mixed ones. The TC of the samples were observed to be significantly greater in the direction of alignment (Table 4b) compared to those that were perpendicular to the direction of alignment (Table 4a). The MWCNT samples at 20 wt% loading exhibited an 11.5-fold increase in TC relative to neat Ultem™ whereas the CNF samples loaded at 30 wt% showed a 15-fold increase. The largest increase was exhibited by 40 wt% loading of EG samples which showed a 38-fold increase. The data indicates that the nanofillers, when aligned, form a network that successfully conducts heat by enabling a more efficient phonon transfer from one filler particle to another. Finally when it comes to the unoriented samples (Table 4c), it was found that 40 wt% CNF filled samples showed a 10-fold increase while the 50 wt% EG sample showed a 19-fold improvement in thermal conductivity. Comparing the neat MWCNTs and the modified MWCNTs, it is observed that TC shows a 100% improvement upon modification. These results prove conclusively that alignment of the nanofillers in the polymer matrix significantly raises the TC of the samples. However, unaligned samples also show a significant improvement and may be useful in applications when it is not possible to process in order to achieve nanoparticles alignment in the desired direction.

4. SUMMARY

Ultem™ 1000 was mixed with three different carbon-based nanofillers in efforts to increase the TC of the polymer. After initial mixing, the nanocomposites were extruded or processed via the LMM process. HRSEM revealed significant alignment of the nanofillers in the extruded samples. TC measurements were made both in the direction and perpendicular to the direction of alignment of nanofillers as well as for unaligned samples. It was found that the largest improvement in TC was achieved in the case of aligned samples when the measurement was performed in the direction of alignment. Unaligned samples also showed a significant improvement in TC and may be useful in applications when it is not possible to align the nanofiller. Modification of MWCNTs leads to double the TC value compared to the composite containing unmodified MWCNTs. However the improvements in TC did not approach those expected based on a rule of mixtures. This is likely due to poor phonon transfer through the matrix.

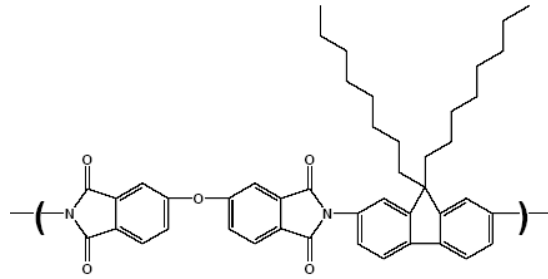# 5. ACKNOWLEDGEMENT

6. FIGURES AND TABLES

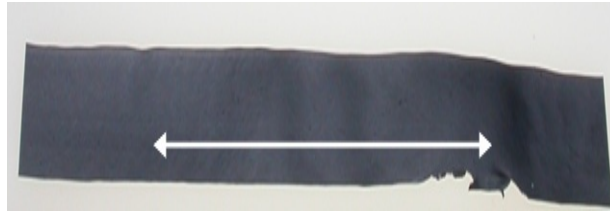Figure 1: Chemical structure of polyimide dispersant

Figure 2: Ribbon of Ultem™/MWCNTs with arrow showing direction of tube alignment
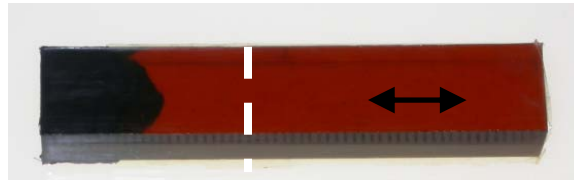

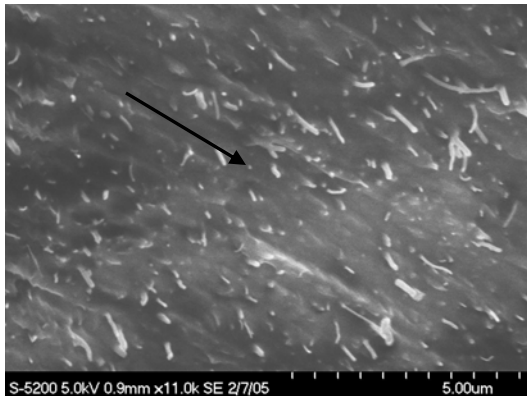Figure 3: Plaque showing cut direction and MWCNTs alignment (arrow)
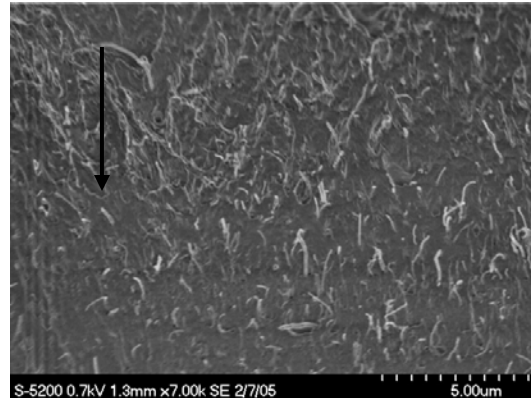

Figure 4(a): Melt mixed

Figure 4(b): Solution mixed

Figure 4: HRSEM of Ultem™/5 wt% MWCNTs ribbon sample; arrow denotes direction of flow
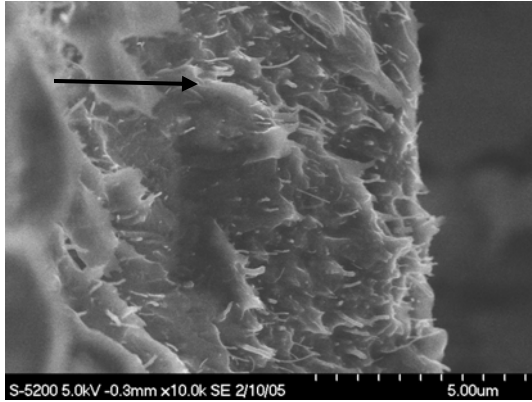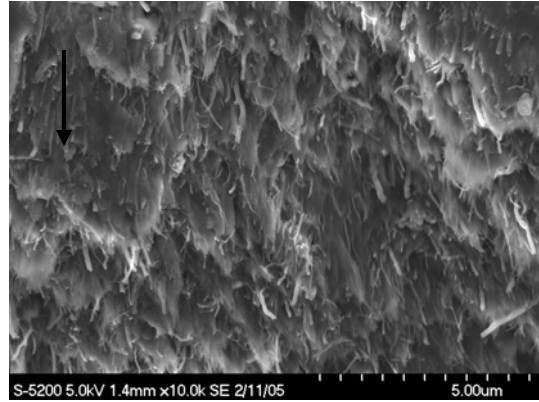
Figure 5(a): 10 wt% MWCNTs melt mixed

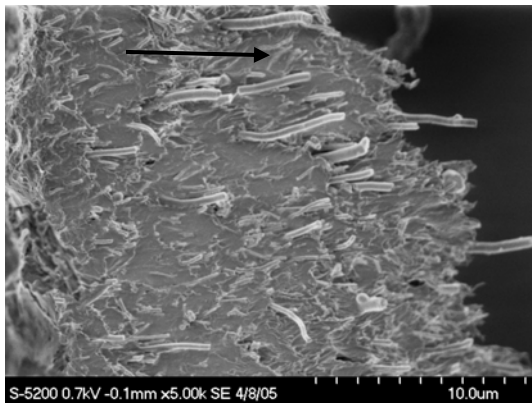
Figure 5(b): 20 wt% MWCNTs melt mixed
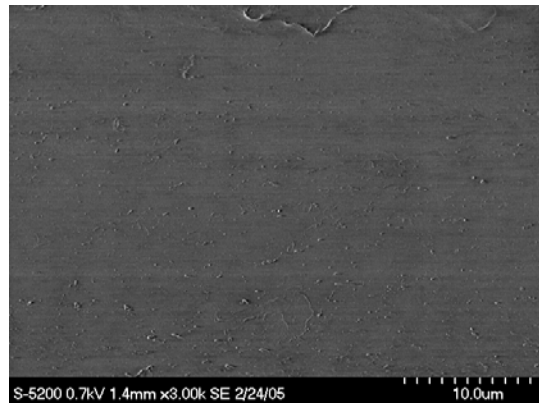

Figure 5(c): 20 wt% CNFs melt mixed

Figure 5(d): 5 wt% MWCNTs melt mixed

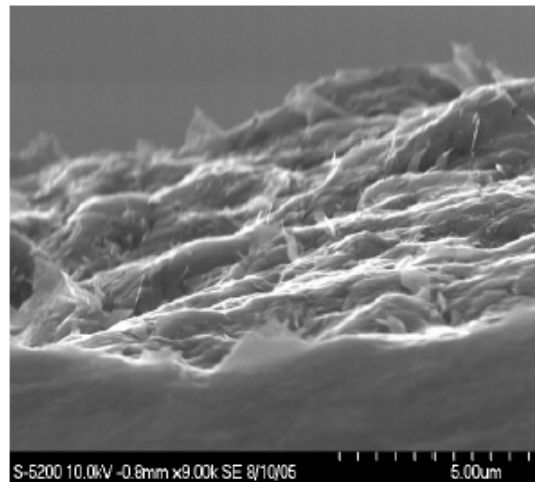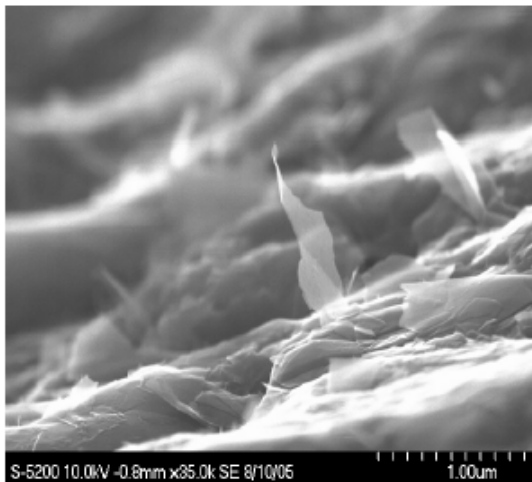Figure 5: HRSEM of Ultem™/nanofiller ribbon sample; arrow denotes direction of flow

Figure 6: 40 wt% Asbury EG in Ultem™ ribbon
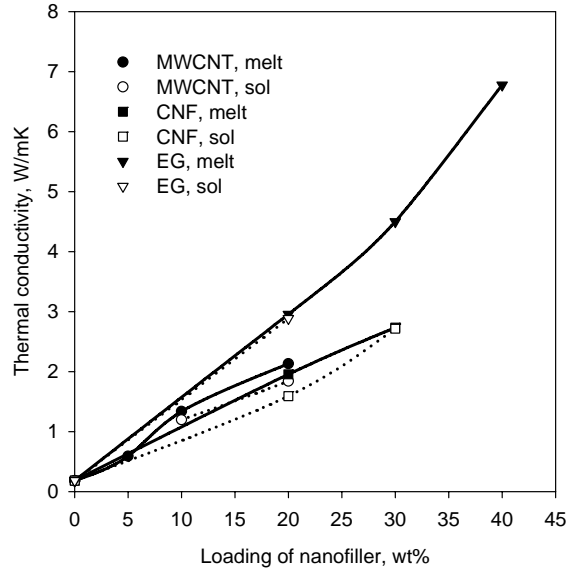
Figure 7: Thermal conductivity of molded Ultem™/nanofiller samples; measurement along direction of alignment

Table 1: Modified MWCNT Characterization

ID	Reaction Conditions	Mass, g		DSC, °C
		Initial	After	
VGE-S12	NA	NA	NA	No transitions observed
A	n-butyllithium @ -78°C then addition of 1-bromododecane.	0.83	0.91	Endotherms at 45 & 113
B	n-butyllithium @ -78°C then 1-bromododecane.	9.02	10.4	1) Endotherms at 99 & 112 2) Endotherms at 86 & 108
C	n-butyllithium @ -78°C.	0.83	0.81	No transitions observed
D	Addition of 1-bromododecane.	0.88	0.86	No transitions observed
E	n-butyllithium @ -78°C then diphenylphosphinic chloride.	0.82	0.85	1) Endotherms at 253 & 258 2) No transitions observed

Table 2: Melt viscosities of Ultem™ 1000/nanofiller samples:

Sample	Viscosity (poise)
Neat Ultem™	37200
Ultem™, 5 wt% MWCNT	38000
Ultem™, 10 wt% MWCNT	47700
Ultem™, 20 wt% MWCNT	54700
Ultem™, 20 wt% CNF	35400
Ultem™, 30 wt% CNF	47200
Ultem™, 40 wt% CNF	50300
Ultem™, 20 wt% EG	31500
Ultem™, 30 wt% EG	37000
Ultem™, 40 wt% EG	46800
Ultem™, 50 wt% EG	57800

Shear rate: 92.5/sec, Temperature: 325 ^{o}C

Table 3: Mechanical properties of Ultem™/nanofiller samples:

Sample	Modulus, GPa	Strength, MPa	Elong., %
Neat Ultem™	1.45 ± 0.05	49.64 ± 1.38	16 ± 11
Ultem™, 5 wt% MWCNT, melt	2.56 ± 0.12	91.70 ± 6.20	7 ± 0.5
Ultem™, 5 wt% MWCNT, sol.	--	--	--
Ultem™, 10 wt% MWCNT, melt	2.95 ± 0.17	72.39 ± 5.51	4 ± 1
Ultem™, 10 wt% MWCNT, sol.	1.19 ± 0.04	31.72 ± 2.07	3.5 ± 0.4
Ultem™, 20 wt% MWCNT, melt	3.50 ± 0.30	60.67 ± 11.72	2 ± .4
Ultem™, 20 wt% MWCNT, sol.	2.05 ± 0.23	58.61 ± 6.20	4 ± 0.5
Ultem™, 20 wt% CNF, melt	2.83 ± 0.30	48.26 ± 6.89	2 ± 0.3
Ultem™, 20 wt% CNF, sol.	2.24 ± 0.04	NA*	NA*
Ultem™, 30 wt% CNF, melt	3.76 ± 0.16	78.60 ± 5.52	3 ± 0.6
Ultem™, 30 wt% CNF, sol.	3.50 ± 0.10	64.12 ± 12.40	2.4 ± 0.7
Ultem™, 20 wt% EG, melt	5.40 ± 0.2	80.00 ± 13.00	2 ± 0.4
Ultem™, 20 wt% EG, sol.	4.70 (1 sample)	80	2.0
Ultem™, 30 wt% EG, melt	7.6 ± 0.3	96.5 ± 19.00	2 ± 0.5
Ultem™, 40 wt% EG, melt	--	--	--

*Ribbons were too thick for the 222.4 N load cell. Only modulus was obtained.

Table 4: T$_g$s of Ultem™/nanofiller samples:

Sample	Melt mixed, T$_g$ (°C)	Solution mixed, T$_g$ (°C)
Neat Ultem™	216 (no mixing)	
Ultem™, 5 wt% MWCNT	217	214
Ultem™, 10 wt% MWCNT	218	198
Ultem™, 20 wt% MWCNT	218	203
Ultem™, 20 wt% CNF	219	218
Ultem™, 30 wt% CNF	218	217
Ultem™, 20 wt% EG	218	217
Ultem™, 30 wt% EG	219	--
Ultem™, 40 wt% EG	219	--

Table 5a: TC of Ultem™/nanofiller extruded ribbons*:

Sample	Thermal Conductivity, W/mK
Neat Ultem™	0.172
Ultem™, 5 wt% MWCNT, melt	0.229
Ultem™, 5 wt% MWCNT, sol.	0.255
Ultem™, 10 wt% MWCNT, melt	0.272
Ultem™, 10 wt% MWCNT, sol.	0.192
Ultem™, 20 wt% MWCNT, melt	0.389
Ultem™, 20 wt% MWCNT, sol.	0.422
Ultem™, 20 wt% CNF, melt	0.364
Ultem™, 20 wt% CNF, sol.	0.386
Ultem™, 30 wt% CNF, melt	0.463
Ultem™, 30 wt% CNF, sol.	0.485
Ultem™, 20 wt% EG, melt	0.248
Ultem™, 20 wt% EG, sol.	0.356
Ultem™, 30 wt% EG, melt	0.287
Ultem™, 40 wt% EG, melt	0.387

*TC measurement is perpendicular to alignment

Table 5b: TC of Ultem™/nanofiller molded samples*:

Sample	Thermal Conductivity, W/mK
Neat Ultem™	0.184
Ultem™, 5 wt% MWCNT, melt	0.592
Ultem™, 5 wt% MWCNT, sol.	broken
Ultem™, 10 wt% MWCNT, melt	1.337
Ultem™, 10 wt% MWCNT, sol.	1.197
Ultem™, 20 wt% MWCNT, melt	2.132
Ultem™, 20 wt% MWCNT, sol.	1.841
Ultem™, 20 wt% CNF, melt	1.955
Ultem™, 20 wt% CNF, sol.	1.592
Ultem™, 30 wt% CNF, melt	2.734
Ultem™, 30 wt% CNF, sol.	2.716
Ultem™, 20 wt% EG, melt	2.956
Ultem™, 20 wt% EG, sol.	2.886
Ultem™, 30 wt% EG, melt	4.499
Ultem™, 40 wt% EG, melt	6.777

* TC measurement is parallel to alignment

Table 5c: TC of Ultem™/nanofiller LMM samples (unoriented):

Sample	Thermal Conductivity, W/mK
Neat Ultem™	0.172
Ultem™, 20 wt% MWCNT, melt	0.500
Ultem™, 20 wt% A, sol	0.804
Ultem™, 20 wt% B, sol	1.068
Ultem™, 20 wt% D, sol	1.087
Ultem™, 20 wt% E, sol	0.904
Ultem™, 40 wt% CNF, melt	1.184
Ultem™, 40 wt% CNF, sol.	1.791
Ultem™, 20 wt% EG, melt	0.585
Ultem™, 30 wt% EG, melt	0.973
Ultem™, 40 wt% EG, melt	2.144
Ultem™, 50 wt% EG, melt	3.174

7. REFERENCES

1. Collister J, Polymer Nanocomposites: Synthesis, Characterization and Modeling, 2002, Ed. R. Krishnamoorti and R.A. Vaia, ACS Symposium Series 804.

2. Hammel E, Tang X, Trampert M, Schmitt T, Mauthner K, Eder A and Potschke P, 2004, *Carbon*, **42**, 1153.

3. Lozano K, Yang S and Zeng Q, 2004, *J. Appl. Poly. Sc.*, **93**, 155.

4. Kuriger RJ, Alam MK, Anderson DP and Jacobsen RL, 2002, *Composites, Part A*, **33**, 53-62.

5. Lozano K, Bonilla-Rios J and Barrera EV, 2001, *J. Appl. Poly. Sc.*, **79**, 125.

6. Carneiro OS, Covas JA, Bernardo CA, Caldeira G, Van Hattum FWJ, Ting JM, Alig RL and Lake ML; 1998, *Composites Sc. Tech.*, **58**, 401.

7. Pogue RT, Ye J, Klosterman DA, Glass AS and Chartoff RP, 1998, *Composites: Part A*, **29**, 1273.

8. Cooper CA, Ravich D, Lips D, Mayer J and Wagner HD, 2002, *Composites Sc. Tech.*, **62**, 1105.

9. Merkulov VI, Lowndes DH, Wei YY, Eres G and Voelkl E, 2000, *Appl Phys Lett*, **76**(24), 3555.

10. Endo M, Kim YA, Hayashi T, Fukai Y, Oshida K, Terrones M, Yanagisawa T, Higaki S and Dresselhaus MS, 2002, *Appl Phys Lett*, **80**(7), 1267.

11. Drzal LT and Fukushima H, Unites States Patent Application Publication, Pub No. US20040127621 (2004).

12. Shen JW, Huang WY, Zuo SW and Hou J, 2005, *J.Appl. Polym. Sc.*, **97**, 51.

13. Zheng W, Lu X and Wong SC, 2004, *J. Appl. Polym. Sc.*, **91**, 2781.

14. Zheng G, Wu J, Wang W and Pan C, 2004, *Carbon*, **42**, 2839.

15. Zheng W, Wong SC and Sue HJ, 2002, *Polymer*, **73**, 6767.

16. Song LN, Xiao M, Li XH and Meng YZ, 2005, *Mater. Chem, Phys.*, **93**, 122.

17. Cho D, Lee S, Yang G, Fukushima H and Drzal LT, 2005, *Macromol. Mater. Eng,* **290**, 179.

18. Gao X, Liu L, Guo Q, Shi J and Zhai G, 2005, *Materials Letters*, **59**, 3062.

19. Lau KT and Hui D, 2002, *Composites Part B: Engineering*, **33**, 263.

20. Park C, Ounaies Z, Watson KA, Crooks RE, Smith Jr. JG, Lowther SE, Connell JW, Siochi EJ, Harrison JS and St. Clair TL, 2002, *Chem. Phys. Lett.*; **364**, 303.

21. Smith Jr. JG, Connell JW and Hergenrother PM, 2001, *Soc. Adv. Matl and Proc. Eng. Proc.*; **46**: 510.

22. Haggenmueller R, Gommans HH, Rinzler AG, Fischer JE and Winey KI, 2000, *Chem Phys Lett;* **330**, 219.

23. Andrews R, Jacques D, Minot M and Rantell T, 2002, *Macromol. Mater. Eng.*, **287**(6), 395.

24. Banerjee S, Hemraj-Benny T and Wong SS, 2005, *Adv. Mater.*, **17**(1), 17.

25. Liu CH, Huang H, Wu Y and Fan SS, 2004, *Appl. Phys. Lett*, **84**, 4248.

26. Kim P, Shi L, Majumdar A and McEuen PL, 2001, *Phys. Rev. Lett.* **87** (21), 215502.

27. Hwang YJ, Ahn YC, Shin HS, Lee CG, Kim GT, Park HS and Lee JK, 2005, *Current Appl. Phys.* article in press (available online August 19, 2005).

28. Choi SUS, Zhang ZG, Yu W, Lockwood FE and Grulke EA, 2001, *Appl. Phys. Lett,* **79**, 2252.

29. Osman MA and Srivastava D, 2001, *Nanotechnology*, **12**, 21.

30. Gong Q, Li Z, Bai X, Li D, Zhao Y and Liang J, 2004, *Mater. Sc. Eng.A* **384**, 209.

31. Shenogin S, Xue L, Ozisik R and Keblinski P, 2004, *J. Appl. Phys.*, **95**(12), 8136.

32. Shenogin S, Bodapati A, Xue L, Ozisik R and Keblinski P, 2004, *Appl. Phys. Lett.*, **85**(12), 2229.

33. Siochi EJ, Working DC, Park C, Lillehei PT, Rouse JH, Topping CT, Bhattacharya AR and Kumar S, 2004, *Composites: Part B*; **35**, 439.

34. Huang H, Liu C, Wu Y and Fan S, 2005, *Adv. Mater (Communications)*, **17**, 1652.

35. Huxtable ST, Cahill DG, Shenogin S, Xue L, Ozisik R, Barone P, Usrey M, Strano MS, Siddons G, Shim M and Keblinski P, 2003, *Nat. Mater.*, **11**, 731.

36. Chen YM and Ting JM, 2002, *Carbon*, **40**, 359.